ORIGINAL ARTICLE

Coming to light: How effective are sediment gravity flows in removing fine suspended carbonate from reefs?

Jaco H. Baas[1] | William Hewitt[1] | Stephen Lokier[2] | James Hendry[3,4]

[1]School of Ocean Sciences, Bangor University, Isle of Anglesey, UK

[2]School of Science, University of Derby, Derby, UK

[3]School of Earth Sciences, University College Dublin, Belfield, Ireland

[4]Iapetus Geoscience Limited, Talaton, Devon, UK

Correspondence
Jaco H. Baas, School of Ocean Sciences, Bangor University, Menai Bridge, Isle of Anglesey, UK.
Email: j.baas@bangor.ac.uk

Abstract

Coral reefs are hard calcified structures, mainly found in warm tropical water. These ecosystems serve important roles as, for example, a source of food, shelter and nursery for different organisms, and in coastal protection. Reef-building organisms have evolved to inhabit a narrow ecological niche and thus are particularly susceptible to rapid changes in their environment, for example, under predicted climate-change scenarios. Anthropogenic climate change is widely accepted as the leading cause of rising ocean temperatures, sea water acidity and sedimentation rate, which all affect a coral's productivity, health and, to some extent, skeletal strength. High-energy weather events, such as storms and hurricanes, can erode reefs, thereby increasing the amount of suspended sediment and consequently the turbidity of the water. The removal of suspended sediment from the reef is vital for the health of reef producers, and a natural process that removes suspended sediment from reefs are sediment gravity flows. A key factor that controls the ability of sediment gravity flows to transport sediment is cohesion, as cohesion determines the run-out distance of a flow through changes in its rheological properties. This study examines the cohesive nature of sediment gravity flows laden with fine-grained $CaCO_3$. These gravity flows laden with mud-grade calcite are compared with flows carrying non-cohesive, silt-sized, silica flour, weakly cohesive kaolinite clay and strongly cohesive bentonite clay, by means of laboratory experiments. The results of these experiments show that the mud-grade calcite flows behave more akin to the silica-flour flows by reaching maximum mobility at considerably higher volumetric suspended sediment concentrations (47% for silica flour and 53% for $CaCO_3$) than the kaolinite and bentonite flows (22% for kaolinite and 16% for bentonite). Fine $CaCO_3$ gravity flows can therefore be regarded as physically non-cohesive, and their high mobility may constitute an effective mechanism for removing suspended sediment from coral reefs, especially at locations where a slope gradient is present, such as at the reef front and forereef. However, biological cohesion, caused by 'sticky' extracellular polymer substances produced by micro-organisms, can render mud-grade calcite cohesive and sediment gravity flows less mobile. The present study

should therefore be seen as a first step towards a more comprehensive analysis of the efficiency of removal of suspended sediment from coral reefs.

1 | INTRODUCTION

Sediment gravity flows (SGFs) are amongst the most important sediment transport processes on Earth, providing large quantities of sediment, carbon, nutrients and pollutants, such as microplastics, to lakes, seas and oceans (Kneller & Buckee, 2000; Postma, 2011; Talling, 2014). In the ocean, SGFs can cause considerable damage to underwater communication cables and other deep-water engineering infrastructure (Talling et al., 2015). Although most research on SGFs has focussed on siliciclastic sediment transport and environments, their deposits are common also in modern and ancient carbonate environments (Austin et al., 1986; Eberli, 1987; Eberli et al., 1997; Swart et al., 2000; Payros & Pujalte, 2008; Betzler et al., 2017; Liu et al., 2023). Yet, process-based research of carbonate-laden gravity flows, and comparisons with siliciclastic gravity flows, is relatively rare (Hodson & Alexander, 2010). A recent paper by Slootman et al. (2023) summarised the present knowledge of the physics of carbonate-sand laden SGFs and analysed the effect of carbonate particle shape and density on their settling velocity in SGFs and their distribution in SGF deposits. Slootman et al. (2023) concluded that 'in addition to grain size and particle density, the irregular shape of skeletal sediments exerts a significant control on the distribution of sand grains in calciturbidites', but their work did not include calciclastic, fine-grained sediment. Below, the term 'mud-grade calcite' is used to describe this sediment in a purely granulometric sense, that is, a mixture of silt and clay-sized CaCO$_3$ particles, without reference to a specific physical, biological or chemical origin (Hubbard et al., 1990).

Fine-grained sediment, including mud-grade calcite, can be cohesive, 'sticky', which has wide-ranging implications for the dynamic behaviour, that is, 'mobility', of SGFs (Marr et al., 2001; Mohrig & Marr, 2003; Sumner et al., 2009; Baas et al., 2009, 2011; Baker et al., 2017), as cohesion works against the gravity-induced principle that flow velocity increases as suspended sediment concentration increases. Particle attraction by cohesion in SGFs can have physical and biological origins (Craig et al., 2020) and these cohesive forces work against turbulent forces to decrease the mobility of SGFs (Baas et al., 2009, 2011). In siliciclastic clay-laden flows, the decrease in mobility may start at a volumetric clay concentration of *ca* 10% (Baker

et al., 2017), although this threshold varies with flow velocity, that is, turbulence intensity; stronger turbulence leads to more breakage of electrostatic bonds between fine particles. Mud-grade calcite consists of fine-grained calcium carbonate that can be entrained, in conjunction with coarser sediment, into the water column in large quantities on carbonate platforms (including reefs) during storms and subaqueous slope failures. This resuspended sediment may then be shed offshore by SGFs (Haak & Schlager, 1989; Reijmer et al., 1992, 2012; and further references in Slootman et al., 2023). The origin of mud-grade calcite can be biological, chemical and detrital (Hubbard et al., 1990; MacDonald & Perry, 2003; Perry et al., 2015; Russ et al., 2015; Trower et al., 2019). The production of mud-grade calcite is a common process on carbonate platforms. However, it is particularly important for unhealthy, brittle reefs subjected to environmental stress, such as coral bleaching. Weakened coral skeletons render these reefs more susceptible to: (a) physical erosion and subsequent production of mud by abrasion of eroded sand and rubble (Trower et al., 2019), (b) biological erosion and production of mud by scrapers and excavators, for example, parrot fish and urchins (Salter et al., 2012; Perry et al., 2015; Russ et al., 2015); (c) cyanobacterial infestation; (d) post-mortem disintegration of calcareous algae; and (e) micro and macroborers, for example, sponges (MacDonald & Perry, 2003; Perry et al., 2015).

Generally, the presence of large volumes of suspended mud is detrimental to carbonate producers and, thus, to sediment production and reef growth (Rogers & Ramos-Scharrón, 2022; Tuttle & Donahue, 2022). Carbonate production is highest in sessile benthic organisms precipitating skeletal material in association with photosynthesis. This process is optimal in shallow clear waters within the uppermost few metres of the photic zone. The presence of mud in the water column reduces the depth of the photic zone and thus reduces the incident light at the sea floor—a process akin to an increase in water depth. Turbidity can have a major impact on gross carbonate production, taphonomy and sediment production of reefs (Mallela & Perry, 2006). Where mud settles onto the reef surface, carbonate producers may be stressed, or even killed, through ingestion or smothering (Lokier et al., 2009; Lokier, 2023).

The aim of this paper is to determine, at first order, how effective SGFs are, in addition to wind, waves and

tides (Lopez-Gamundi et al., 2024), in shedding fine suspended $CaCO_3$ sediment off reefs, considering that removal of suspended sediment from the water column above reefs is needed to clear turbid water and aid the maintenance of reef health (Jones et al., 2020). Experimental research was used to compare the head velocity, run-out distance and deposit shape of flows laden with mud-grade calcite (crushed limestone) with non-cohesive siliciclastic silt flows and cohesive siliciclastic clay flows. This comparison aims to derive a descriptive measure of the degree of cohesion of SGFs laden with mud-grade calcite. The hypothesis is that, if fine $CaCO_3$ flows are non-cohesive, the low settling velocity of the mud-grade calcite renders these flows highly mobile and well able to remove suspended sediment from reefs after storms. The specific objectives of this research are therefore:

1. to determine if SGFs laden with mud-grade calcite (crushed limestone) are physically cohesive or non-cohesive;
2. to quantify changes in mobility of mud-grade calcite SGFs and deposit shape as a function of suspended $CaCO_3$ concentration;
3. to discuss differences between healthy and unhealthy, brittle reefs in the efficiency of $CaCO_3$-laden flows to clean turbid water, especially after storms;
4. to consider the potential effect of biological cohesion and particle shape and density on the mobility of SGFs laden with mud-grade calcite in view of future research.

2 | BACKGROUND AND RATIONALE

2.1 | Coral reefs

Coral reefs are amongst the largest and most complex ecosystems on Earth, primarily found in warm waters in the tropics (Spalding, 2001). Most reef-forming scleractinian corals host symbiotic dinoflagellate zooxanthellae that use light to provide nutrients to the coral (Berkelmans & van Oppen, 2006). Millions of species worldwide call reefs their home (Sheppard et al., 2017) and an estimated six million people around the globe are dependent on coral reefs (Cinner, 2014). Reefs supply job opportunities to local communities and they provide a food source and recreational opportunities, such as diving and eco-tourism (Costanza et al., 2014). Reefs also support coastal communities by providing protection against coastal hazards. As such, coral reefs act like sandbars and barrier islands by dispersing wave energy from storms and hurricanes (Spalding et al., 2014).

Because of the delicate relationship with zooxanthellae, coral reefs are sensitive to outside stressors, such as heat, acidification and sedimentation. Coral species, in particular, are susceptible to change. If the external stressors become too strong, the zooxanthellae are expelled from the coral, leaving them colourless (bleached). The world's oceans have been warming since the start of the industrial revolution, in parallel with the increase of atmospheric carbon. Carbon dioxide gas traps heat close to the Earth surface, with the oceans serving as a heat sink (Stocker et al., 2013). The increased sea water temperature negatively affects the health of coral reefs, which can only thrive within a narrow water temperature range (Wilson, 2012). A direct consequence of rising oceanic CO_2 levels is ocean acidification. This happens when sea water and CO_2 mix to make CO_3^{2-} (carbonate), HCO_3^- (bicarbonate) and H^+ (hydrogen), which lowers the pH. As a result of ocean acidification, corals cannot produce calcium carbonate as easily (Langdon & Atkinson, 2005). Reefs that have undergone bleaching because of rising sea water temperature and possibly also ocean acidification are more delicate than healthy reefs (Anthony et al., 2008). In the period between 1980 and 2016, the years 1998, 2005, 2010 and 2016 had particularly high numbers of bleaching events around the world (Hughes et al., 2018). Without a strong calcified outer layer, a coral is more susceptible to physical and biological erosion (MacDonald & Perry, 2003; Perry et al., 2015; Russ et al., 2015; Trower et al., 2019). Reefs in the tropics suffer regular high-energy events, as hurricane-generated waves and storm surges are common at these latitudes. During these events, corals as far down as 20 m can be affected, with certain growth forms, such as branching corals, being particularly susceptible (Scoffin, 1993). It is therefore hypothesised that an unhealthy, brittle reef produces more suspended sediment, including mud-grade calcite via abrasion of sand and gravel (Trower et al., 2019), during a storm or hurricane than a stronger, more calcified, healthy reef. The problem is compounded by the fact that reefs that have been affected by natural or anthropogenic disturbances exhibit slower coral recovery rates under higher turbidity conditions (Evans et al., 2020). Moreover, anthropogenic eutrophication causes a change in the balance of coral versus coralline algae within the reefs (Chazottes et al., 2008), which further exacerbates the production of large amounts of mud-grade carbonate sediment by, in particular, biological erosion.

The amount of sediment input to reefs from anthropogenic sources, such as remobilisation by fishing and dredging, has increased substantially (Brodie & Pearson, 2016). High levels of suspended sediment above and around coral reefs make the water more turbid,

reducing the light penetration to the corals and hindering photosynthesis and zooxanthellae productivity (Rogers, 1990). Sediment settling on coral tissue causes further shading and smothering. Healthy corals can actively remove small amounts of sediment from their tissues via ciliary activity, hydrostatic expansion, tentacle movements and mucus production (Brunner, 2021), but unhealthy corals are less able to do so. Shading and smothering contribute to a further decrease in the productivity of the photosynthesising zooxanthellae; this is another major cause of coral bleaching (Erftemeijer et al., 2012). Where smothering is significant, corals and other sessile benthic carbonate producers are killed through anoxia or tissue necrosis (references in Lokier, 2023). Even small amounts of smothering may kill carbonate producers because an inability to feed results in starvation. Calcification rates are three times higher in light conditions than in dark conditions, and recent studies have suggested that calcification is dark-repressed rather than light-enhanced (Venn et al., 2019). Thus, a coral reef in sea water with high amounts of suspended sediment calcifies less (Gattuso et al., 1999). This lower calcification rate results in the construction of a weaker skeleton and higher vulnerability of the reef to biological erosion (MacDonald & Perry, 2003; Perry et al., 2015; Russ et al., 2015) and mechanical breakdown during storms (Crook et al., 2013). In turn, more suspended sediment needs to be transported away from the reef after storm events to ensure coral productivity and health.

2.2 | Sediment gravity flows

Sediment gravity flows are known to shed suspended sediment off reefs into deeper water (Haak & Schlager, 1989; Reijmer et al., 1992, 2012; and further references in Slootman et al., 2023), but SGFs vary significantly in their efficiency of sediment transport, that is, in flow mobility. The controls on the mobility of SGFs can be summarised by four main factors: (1) flow type, which can be laminar, transitional or turbulent; (2) flow behaviour, which can be cohesive or non-cohesive; (3) excess density of the flow relative to the ambient water; and (4) substrate slope gradient (Talling et al., 2012). The present paper focusses on cohesion and excess density, here expressed as volumetric sediment concentration. Depending on flow type and rheology, SGFs can behave as fluid or plastic. Examples of fluidal flows used in this paper are low-density and high-density turbidity currents (Baker et al., 2017). Mud flows and slides, also used in this paper, are examples of plastic flow (Baker et al., 2017).
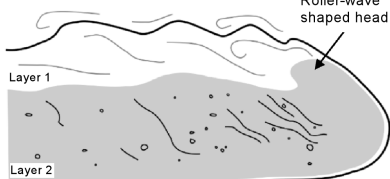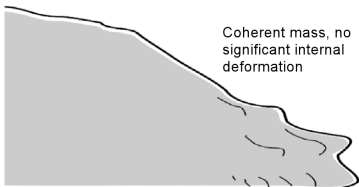
Following the definitions of Baker et al. (2017), low-density turbidity currents are fully turbulent, that is, well-mixed flows without an internal density interface (Figure 1; Baker et al., 2017). High-density turbidity currents (Baker et al., 2017) have two distinct layers: a low-density, fully turbulent cloud of suspended sediment in the upper part separated by a density interface from a high-density layer with reduced turbulence in the lower part of the flow (Figure 1). Mud flows are defined as high-concentration, laminar SGFs without significant internal turbulence, in which a cohesive clay gel provides grain support by matrix strength (Middleton & Hampton, 1973; Baker et al., 2017). Mud flows may have a dilute top, caused by minor mixing with the ambient water. A slide is a coherent mass flow without significant internal deformation, formed at the highest suspended sediment concentrations (Figure 1; Baker & Baas, 2023).

2.3 | Cohesion

Sediment gravity flows can be subdivided in non-cohesive, dominantly fluidal flow types and cohesive, dominantly plastic flow types. Cohesive SGFs are more complex than non-cohesive SGFs, because of the ability of clay particles to form aggregates (floccules) and gels (Mehta et al., 1989). The presence of floccules and gels increases the viscosity and yield strength and modulates the turbulence maintaining the flow (Baas & Best, 2002). Floccule size generally increases as bulk suspended clay concentration increases (Dyer & Manning, 1999) until a gelling point is reached, at which a volume-filling network of clay particle bonds in the liquid, a gel, establishes.

Settling of clay particles is dependent on the concentration—and less so on the size—of individual clay particles if the settling is controlled by the aggregation and gelling processes (Dyer & Manning, 1999). In low-concentration suspensions, in which flocs are small, the settling velocity and concentration are independent of each other. However, in high-concentration suspensions, particles are more likely to form large flocs, which usually have a greater submerged weight, and therefore a higher settling velocity (Dyer & Manning, 1999). Clay gelling inhibits the turbulence of the flow through increased viscosity (Baker et al., 2017). Flows that behave as a gel tend to deposit 'en masse'. This bulk settling process involves a positive feedback mechanism, 'cohesive freezing' (Mulder & Alexander, 2001). Cohesive freezing typically follows a reduction in the head velocity of the flow, which decreases turbulent forces, allowing the clay minerals to form a greater number of electrostatic bonds, in turn increasing cohesive strength. This then further reduces the turbulence and results in a rapid further reduction in the

FIGURE 1 Generic sediment gravity flow type classification scheme of Baker et al. (2017) applied to the CaCO₃-laden flows used in this study (modified after Baker & Baas, 2023).

head velocity of the flow. This deceleration process repeats itself until the flow swiftly comes to a halt. The equivalent process in non-cohesive, usually silt-laden, SGFs is 'frictional freezing'. Frictional freezing takes place at considerably higher sediment concentrations than cohesive freezing, because non-cohesive particles do not form gels (Baker et al., 2017).

2.4 | Research approach

In order to estimate how effectively fine suspended CaCO₃ sediment can be transported by SGFs, lock-exchange experiments were conducted with mud-grade calcite gravity flows. The experiments comprised a full range of initial suspended sediment concentrations, covering low-density and high-density turbidity currents, mud flows and slides (sensu Baker et al., 2017; Figure 1). The observation that flows carrying fine non-cohesive siliciclastic particles (silica flour in Table 1) are highly mobile up to volumetric concentrations of 52% and equivalent cohesive SGFs lose mobility at much lower concentrations, for example, at 20% for bentonite clay (Table 1; Baker et al., 2017), allows us to estimate the cohesive properties of the mud-grade calcite flows through comparison of head velocity, run-out distance and deposit shape. This follows procedures used by Craig et al. (2020), Sobocinska and Baas (2022) and Baker and Baas (2023) for siliciclastic sediment. In turn, this information is used to discuss how effective mud-grade calcite SGFs can be in cleaning turbid water above reefs, primarily based on the degree of cohesion, but also taking other controls on flow mobility, such as biological cohesion, into consideration.

3 | METHODS AND MATERIALS

Fifteen lock-exchange experiments were conducted in the Hydrodynamics Laboratory of Bangor University (NW Wales, UK) between October 2022 and February 2023. The lock-exchange tank is 5 m long, 0.2 m wide and 0.5 m deep (Figure 2). It is made up of two sections: a 0.31 m long reservoir separated from the 4.69 m long main body by a lock gate. The slope of the tank was set to 0° in all experiments to allow direct comparison with the siliciclastic flows studied by Baker et al. (2017), to minimise the number of variables and to achieve a minimum requirement for mud removal, as slopes promote flow and favour turbulent driving forces over mobility-reducing cohesive forces. For each experiment, the reservoir was filled with a mixture of sea water and fine-grained calcium carbonate particles to a depth of 0.35 m (Figure 2). The

TABLE 1 Summary of experimental data of this study (mud-grade calcite) and Baker et al. (2017) (kaolinite, bentonite, silica flour).

Sediment type	Initial sediment concentration (%)	Run-out distance (m)	Maximum head velocity (m s^{-1})	Flow type
Mud-grade calcite	1	4.69[a]	0.108	LDTC
Mud-grade calcite	5	4.69[a]	0.239	LDTC
Mud-grade calcite	10	4.69[a]	0.330	LDTC
Mud-grade calcite	15	4.69[a]	0.404	LDTC
Mud-grade calcite	20	4.69[a]	0.504	LDTC
Mud-grade calcite	25	4.69[a]	0.572	LDTC
Mud-grade calcite	30	4.69[a]	0.657	LDTC
Mud-grade calcite	35	4.69[a]	0.696	LDTC
Mud-grade calcite	40	4.69[a]	0.796	LDTC
Mud-grade calcite	45	4.69[a]	0.851	LDTC
Mud-grade calcite	50	4.69[a]	0.801	HDTC
Mud-grade calcite	53	3.75	0.781	HDTC
Mud-grade calcite	55	2.74	0.727	HDTC
Mud-grade calcite	58	1.16	0.551	Mud flow
Mud-grade calcite	59	0.75	0.445	Slide
Silica flour	1	4.69[a]	0.11	LDTC
Silica flour	5	4.69[a]	0.24	LDTC
Silica flour	10	4.69[a]	0.34	LDTC
Silica flour	15	4.69[a]	0.45	LDTC
Silica flour	25	4.69[a]	0.58	LDTC
Silica flour	40	4.69[a]	0.69	LDTC
Silica flour	44	4.69[a]	0.71	LDTC
Silica flour	46	4.69[a]	0.75	HDTC
Silica flour	47	4.66	0.75	HDTC
Silica flour	48	3.68	0.71	HDTC
Silica flour	49	2.82	0.71	HDTC
Silica flour	50	1.53	0.64	HDTC
Silica flour	51	0.96	0.61	Mud flow
Silica flour	52	0.49	0.29	Slide
Kaolinite clay	1	4.69[a]	0.11	LDTC
Kaolinite clay	5	4.69[a]	0.28	LDTC
Kaolinite clay	10	4.69[a]	0.33	LDTC
Kaolinite clay	15	4.69[a]	0.41	LDTC
Kaolinite clay	22	4.35	0.50	HDTC
Kaolinite clay	23	3.66	0.48	HDTC
Kaolinite clay	25	2.09	0.48	HDTC
Kaolinite clay	27	1.01	0.40	Mud flow
Kaolinite clay	29	0.45	0.29	Slide
Bentonite clay	1	4.69[a]	0.1	LDTC
Bentonite clay	5	4.69[a]	0.23	LDTC
Bentonite clay	10	4.69[a]	0.31	LDTC
Bentonite clay	15	4.66	0.35	HDTC
Bentonite clay	16	3.77	0.37	HDTC

TABLE 1 (Continued)

Sediment type	Initial sediment concentration (%)	Run-out distance (m)	Maximum head velocity (m s^{-1})	Flow type
Bentonite clay	17	3.12	0.34	HDTC
Bentonite clay	18	1.42	0.27	Mud flow
Bentonite clay	19	1.22	0.22	Mud flow
Bentonite clay	20	0.22	0.07	Slide

Abbreviations: LDTC, low-density turbidity current; HDTC, high-density turbidity current.

[a]Minimum run-out distance.

FIGURE 2 Experimental setup used for the lock-exchange tank experiments. The tank is 0.2 m wide and the slope of the tank was set to 0° in all experiments (after Baker et al. 2017).
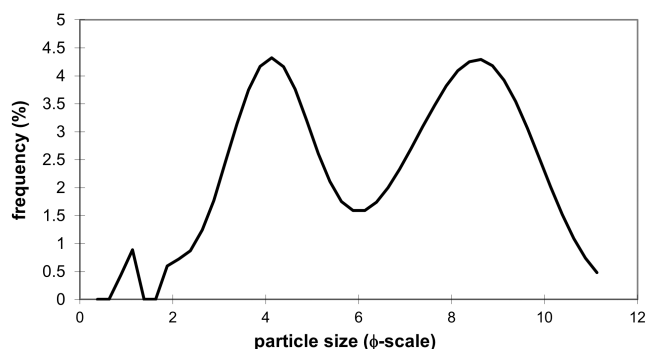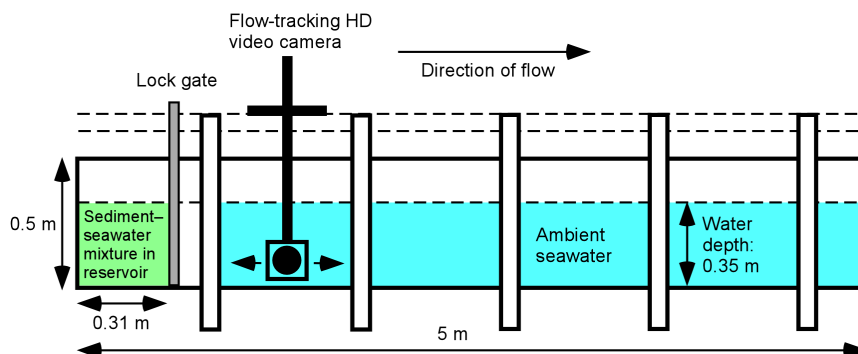

FIGURE 3 Frequency distribution curve of the particle size of the mud-grade calcite used in the experiments. Particle size is given in φ(phi)-values.

remainder of the tank was filled simultaneously with sea water to the same level as in the reservoir. The sea water was sourced from the Menai Strait (NW Wales, UK) and filtered to remove suspended particles before application. The salinity and temperature of the sea water were 35 psu and *ca* 15°C, respectively. As a first-order approximation of natural mud-grade calcite, the calcium carbonate used in the experiments consists of crushed limestone (calcite) without significant intra-particle porosity, manufactured by Omya® (C.A.S. number 1317-65-3) and supplied under the name 'Calcium Carbonate Powder' by Elixir Garden Supplies in the UK. The size distribution of the mud-grade calcite was measured using a Microtrac Sync laser particle sizer at the School of Ocean Sciences, Bangor University. The mud-grade calcite is a very poorly sorted sandy mud with a median size of 0.009 mm (6.9φ: fine silt) and a sorting coefficient of 2.466 (Folk & Ward, 1957). Figure 3 shows two main modal sizes at 0.0025 mm (8.6φ: clay) and 0.060 mm (4.1φ: coarse silt). The volumetric concentration of CaCO$_3$ in the flows ranged from 1 to 59%.

A consistent method was used to prepare each mixture of sea water and mud-grade calcite to account for any settling and time-dependent rheological behaviour. Volumetric suspended sediment concentrations were determined from the density, ρ and required mass of CaCO$_3$ and sea water, with $\rho_{\text{mud-grade calcite}} = 2710 \text{ kg m}^{-3}$ and $\rho_{\text{seawater}} = 1027 \text{ kg m}^{-3}$. The total volume of the mixture was 0.02446 m^3. This was sufficient to fill the reservoir to a depth of 0.4 m, thus allowing for some loss of the mixture during preparation. Dry CaCO$_3$ and sea water were mixed for 10 min in a concrete mixer. Thereafter, the suspension was decanted in a container and the walls of the mixer were scraped down to ensure that as little as possible of the mixture was left in the mixer. The suspension was then mixed with a handheld mixer for a further 3 min to make sure the mixture was free of lumps. Subsequently, the mixture was transferred to the reservoir whilst the main body of the tank filled with sea water, to avoid leakage because of pressure differences between both sides of the lock gate. Immediately before lifting the gate and starting an experiment, the mixture in the reservoir was homogenised for 60 s with the handheld mixer. A HD video camera, attached

to runners on top of the tank, tracked the front of the flow along the tank. The video recordings (Video S1) were used to describe and classify the SGFs (cf., Baker et al., 2017; Figure 1) and determine the mean velocity of the head of the flow at each 0.1 m distance along the flow path, as well as the run-out distance of flows that did not reach the end of the tank. Deposit thicknesses were measured with electronic callipers and rulers, but only for flows that did not reflect off the end wall, as these reflections disturbed the deposits. Maximum head velocity of the flows along the tank is used throughout this paper to allow a comparison with previous work on siliciclastic silt and clay flows.

4 | RESULTS

The experimental data for the mud-grade calcite experiments are summarised in Table 1, which also shows the experimental results of Baker et al. (2017) for kaolinite clay, bentonite clay and silica flour that were conducted using the same method. Figure 4 depicts the heads of selected mud-grade calcite flows. Figure 5 shows changes in head velocity with distance along the tank for all flows, and Figure 6 summarises changes in deposit thickness with distance along the tank.

4.1 | Visual observations

The videos reveal that the 1–45% mud-grade calcite flows were all fully turbulent between base and top (Figure 4A,B) and had a semi-elliptically shaped head and distinct Kelvin–Helmholtz instabilities at their upper boundary in vertical cross-section parallel to the flow direction. These flows kept their forward momentum to the end of the tank, suggesting that the turbulence in these flows was able to outcompete the particle settling and kept most particles in suspension until the flows reflected off the end wall. These properties match the low-density turbidity current type of Baker et al. (2017) (Figure 1).

The flows laden with 50, 53 and 55% mud-grade calcite had two distinct parts separated by a density interface (dashed white line in Figure 4C,D). The upper part of these flows had a relatively light colour and mixed freely with the ambient sea water, whereas the lower part of these flows was darker, denser and undisturbed by the sea water (Figure 4C,D). The flow front was more circular in vertical cross-section parallel to the flow direction than for the low-density turbidity currents. The flows laden with 50, 53 and 55% mud-grade calcite are classified as high-density turbidity currents (cf., Baker et al., 2017; Figure 1).

FIGURE 4 Video stills of the heads of selected CaCO$_3$ flows. (A) 15% low-density turbidity current, (B) 25% low-density turbidity current, (C) 53% high-density turbidity current, (D) 55% high-density turbidity current, (E) 58% mud flow and (F) 59% slide. Dashed lines in (C) and (D) show density interfaces in high-density turbidity currents. Arrow in (E) points to lip region of mud flow. Scale bar is 100 mm long.
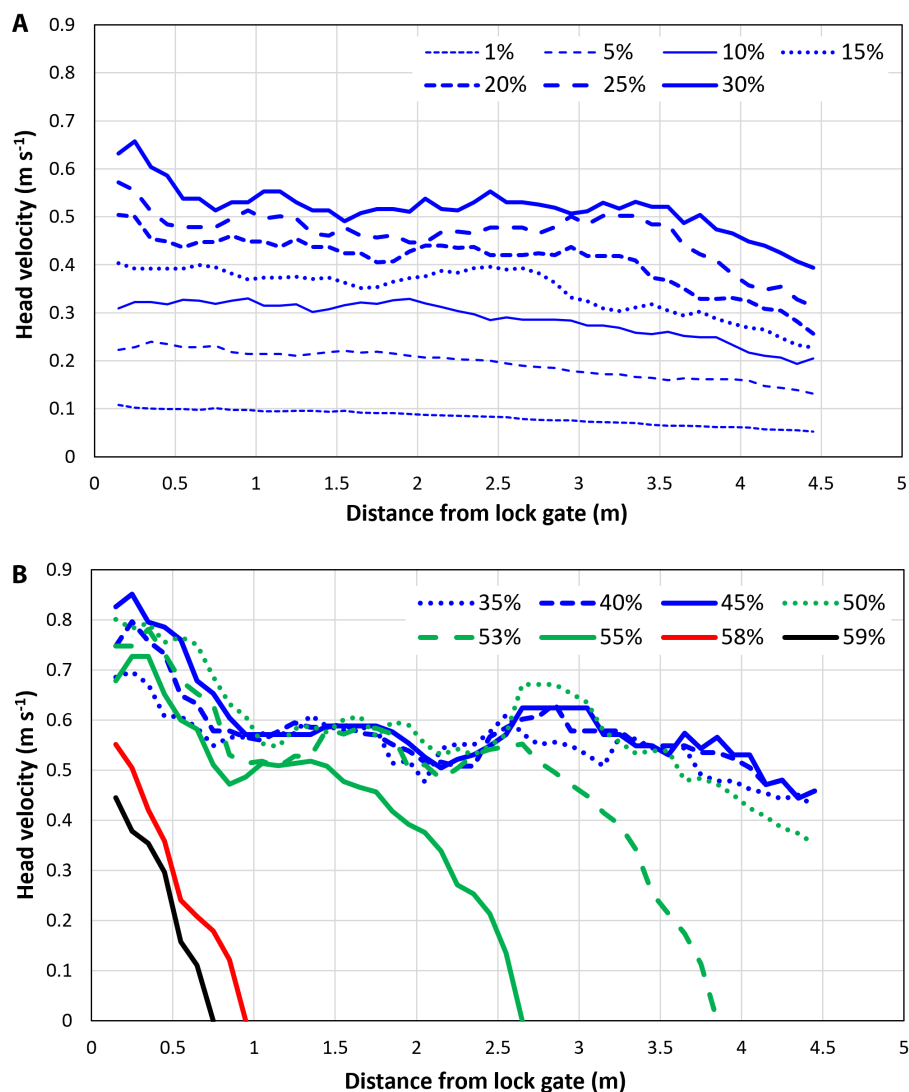
FIGURE 5 Head velocity plotted against downflow distance from the lock gate for: (A) 1–30% mud-grade calcite flows; and (B) 35–59% mud-grade calcite flows. Low-density turbidity currents, high-density turbidity currents, mud flows and slides are given in blue, green, red and black, respectively.

FIGURE 6 Deposit thickness trends of mud-grade calcite flows that had a measurable run-out distance. High-density turbidity currents, mud flow and slide are given in green, red and black, respectively.
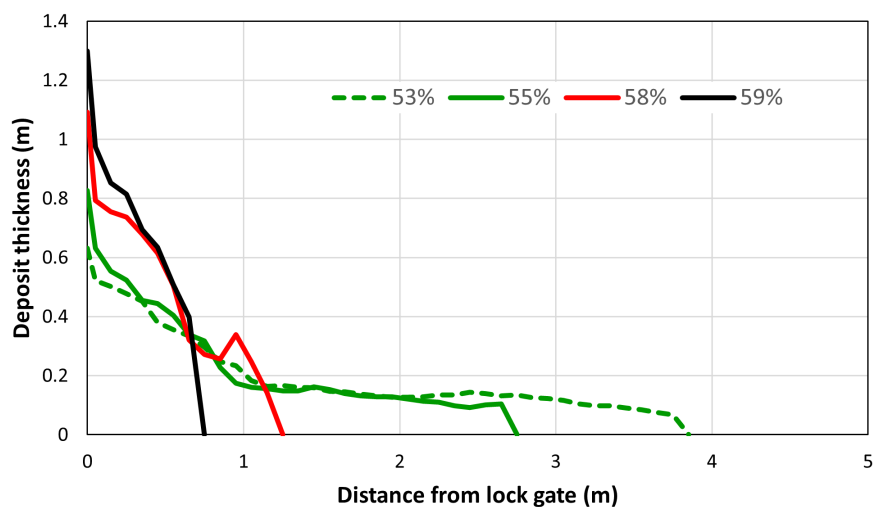
The flow laden with 58% mud-grade calcite had a characteristic lip at the top of the head (white arrow in Figure 4E). The flow lacked internal mixing and minor mixing with the ambient water resulted in a dilute suspension cloud near the top of the flow. The head of the 58% flow had a pointed shape and was lifted off the floor of the tank by incursion of sea water underneath the base of the flow, that is, the flow hydroplaned. These characteristics match the mud-flow type of Baker et al. (2017).

The flow laden with 59% mud-grade calcite was wedge-shaped and it lacked internal deformation. Mixing with the ambient sea water was negligible. The flow mobility was low and most of the sediment was deposited close to the lock gate (Figure 6). This flow is classified as a slide (cf., Baker et al., 2017).

4.2 | Head velocity

Figure 5 shows how the head velocity of each mud-grade calcite flow changed with increasing distance, x, from the lock gate. The initial head velocity, at $x = 0.15\,\text{m}$, increased from $0.11\,\text{m}\,\text{s}^{-1}$ for the 1% flow to $0.63\,\text{m}\,\text{s}^{-1}$ for the 45% flow (Figure 5B). As these low-density turbidity currents travelled along the tank, their head velocity decreased to $0.053\,\text{m}\,\text{s}^{-1}$ for the 1% flow, $0.39\,\text{m}\,\text{s}^{-1}$ for the 30% flow (Figure 5A) and $0.46\,\text{m}\,\text{s}^{-1}$ for the 45% flow (Figure 5B). All ≤45% flows reflected off the end of the tank, so they had a minimum run-out distance of 4.69 m.

In contrast to the low-density turbidity currents, the initial head velocity decreased as the concentration of mud-grade calcite was increased from 50 to 59%: from $0.80\,\text{m}\,\text{s}^{-1}$ for the high-density turbidity current laden with 50% mud-grade calcite, via $0.55\,\text{m}\,\text{s}^{-1}$ for the mud flow carrying 58% mud-grade calcite, to $0.44\,\text{m}\,\text{s}^{-1}$ for the slide laden with 59% mud-grade calcite (Figure 5B). The 50% high-density turbidity current decelerated quicker than the low-density turbidity currents near the end of tank but still maintained a head velocity of $0.35\,\text{m}\,\text{s}^{-1}$ close to the end wall. The 53 and 55% high-density turbidity currents, 58% mud flow, and 59% slide stopped before reaching the end of the tank and did so progressively closer to the lock gate (Figure 5B). These flows therefore had measurable run-out distances, decreasing from 3.75 to 0.75 m, as the concentration of mud-grade calcite was increased (Table 1).

4.3 | Deposit properties

Figure 6 shows the deposits of all mud-grade calcite flows that had a measurable run-out distance. The length of the deposits decreased, and their maximum thickness increased, as concentrations of mud-grade calcite increased from 53 to 59%. The 53% high-density turbidity current produced a relatively thin deposit with a length of 3.75 m, whereas the 59% slide produced a thick and short deposit that extended into the tank by only 0.75 m. The deposit shape of the high-density turbidity currents was different from that of the mud flow and slide. The high-density turbidity current deposits thinned rapidly in the first metre, after which the thickness was approximately constant for up to 3 m. The deposits then terminated abruptly. The mud flow and slide deposits are characterised by more linear and more rapid thinning than the high-density turbidity current deposits.

5 | DISCUSSION

5.1 | Is mud-grade calcite cohesive?

Figure 7 depicts the maximum head velocity of the experimental flows as a function of concentration of mud-grade calcite, and compares these with the strongly cohesive bentonite clay, weakly cohesive kaolinite clay and non-cohesive silica-flour flows of Baker et al. (2017). The maximum head velocity of the mud-grade calcite flows gradually increased as the initial suspended sediment concentration was increased from 1 to 45%, because increasing the concentration of $CaCO_3$ increased the density contrast between the flow and the ambient fluid. This excess density, together with turbulence, are the drivers of these low-density turbidity currents. Despite the higher excess density in the mud-grade calcite laden high-density turbidity currents, mud flow and slide, the maximum head velocity decreased rapidly as the sediment concentration was increased from 50 to 59% (Figure 7).

The shape of the maximum head velocity curve for mud-grade calcite matches that of bentonite, kaolinite and silica flour, but the mud-grade calcite curve is closest in terms of maximum mobility, that is, peak maximum head velocity, to the silica-flour curve (Figure 7). This peak is at 45% for mud-grade calcite and at 47% for silica flour, whereas the peaks for bentonite and kaolinite are at 16 and 22%, respectively. As silica flour is non-cohesive, and kaolinite and bentonite are cohesive (Baker et al., 2017), this suggests that the mud-grade calcite flows behaved in a non-cohesive manner and can reach significantly higher mobilities at higher concentrations than cohesive clay flows (Figure 7). The decrease in maximum head velocity between 50 and 59% mud-grade calcite therefore probably results from attenuation of turbulence by frictional forces between the $CaCO_3$ particles within the flow, rather than
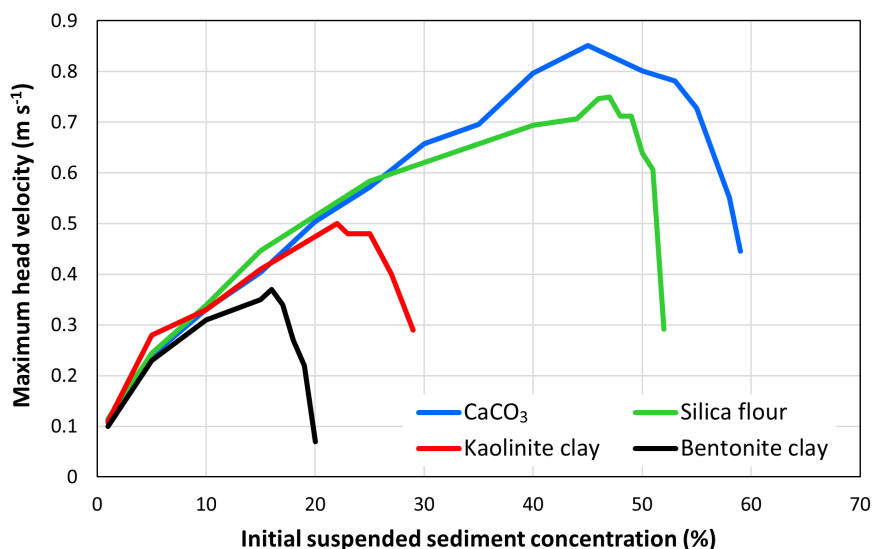
FIGURE 7 Maximum head velocity of CaCO₃, kaolinite, bentonite and silica-flour flows plotted against initial suspended sediment concentration.

cohesive forces (which do not require particles to 'rub' against each other). The fact that these concentrations are close to the random packing density of spheres in deposits of 60% (loose random packing) to 64% (close random packing), when a pervasive network of particle contacts is present and thus the frictional strength is highest, supports this interpretation. The inference that the mud-grade calcite SGFs were non-cohesive, behaving in a similar way to the non-cohesive silica-flour SGFs of Baker et al. (2017), is supported further by similar trends in run-out distance (Figure 8) and deposit shape (Figure 9). The bentonite and kaolinite clay flows started to run out and change deposit shape at much lower concentrations than the silica-flour and mud-grade calcite flows (Figure 8).

Figure 7 reveals also that the mud-grade calcite flows were more mobile than the silica-flour flows at concentrations above *ca* 30%. The mud-grade calcite flows reached a higher peak maximum head velocity than the silica-flour flows (0.85 vs. 0.75 m s^{-1}) and frictional forces slowed down the silica-flour flows at lower concentrations than the mud-grade calcite flows. Moreover, matching run-out distances and deposit shapes are associated with higher mud-grade calcite than silica-flour concentrations in high-density turbidity currents, mud flows and slides (Figure 8). This confirms that the high-concentration, turbulence-attenuated, mud-grade calcite flows were more mobile than the silica-flour flows.

The comparison with Baker et al. (2017) in Figures 7, 8 and 9 shows that the mud-grade calcite flows were non-cohesive, yet somewhat more mobile than non-cohesive silica-flour flows under turbulence-attenuated conditions. Although silica flour was deemed to be non-cohesive by Parker (1987), Pashley and Karaman (2004) suggested that silica-flour particles have weak negative surface charges. Silica flour may therefore be weakly cohesive—but considerably weaker than kaolinite—possibly explaining the lower mobility of silica-flour laden high-density turbidity currents, mud flows and slides compared to the equivalent mud-grade calcite flow types. However, this inferred higher mobility of mud-grade calcite flows may be partly counteracted by the presence of weak surface charges of CaCO₃ particles in electrolytic solutions, such as sea water (Eriksson et al., 2007). Alternative explanations for the difference in mobility between the high-concentration silica-flour and mud-grade calcite SGFs are differences in median particle size (0.018 and 0.009 mm, respectively), particle size distribution (poorly sorted and very poorly sorted, respectively) and particle shape (Slootman et al., 2023). Further research is needed to determine the effect of these parameters on differences in flow mobility for siliciclastic and calciclastic sediment, especially in dense, turbulence-modulated flows.

5.2 | Wider implications

Our laboratory experiments provide a fundamental physical understanding of the dynamics of SGFs that carry fine-grained CaCO₃. The experimental data suggest that these flows are highly mobile up to concentrations that approach the packing density of deposits, because mud-grade calcite is physically non-cohesive and frictional forces are needed to reduce flow mobility. Since the experiments isolated a single parameter, physical cohesion, a detailed comparison with dynamically more complex natural SGFs on coral reefs is not possible yet. Natural flows can be faster than the SGFs simulated herein, in which case the changes in flow type, for example, from low-density to high-density turbidity current, should occur at even higher suspended sediment concentrations than found in this study. It is therefore
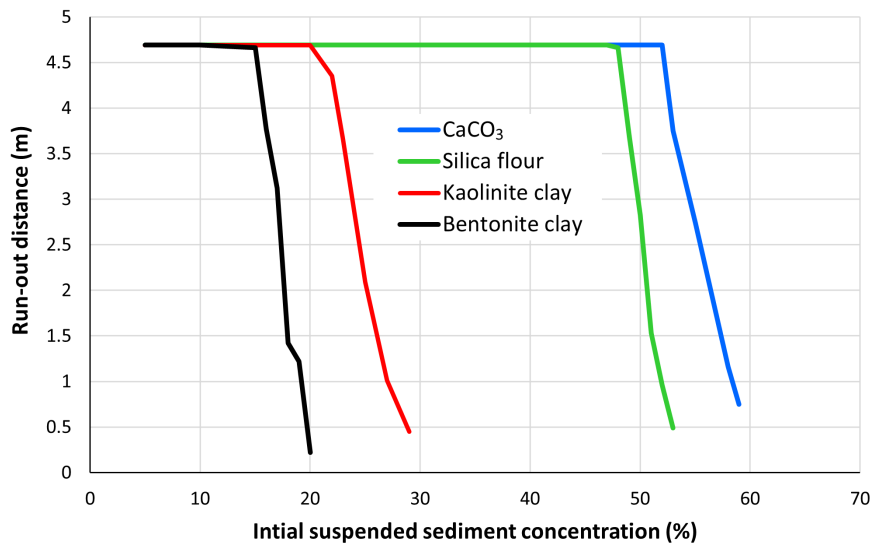
FIGURE 8 Run-out distance of $CaCO_3$, kaolinite, bentonite and silica-flour flows plotted against initial suspended sediment concentration. Run-out distances of 4.69 m denote minimum values; these flows reflected off the end of the tank.
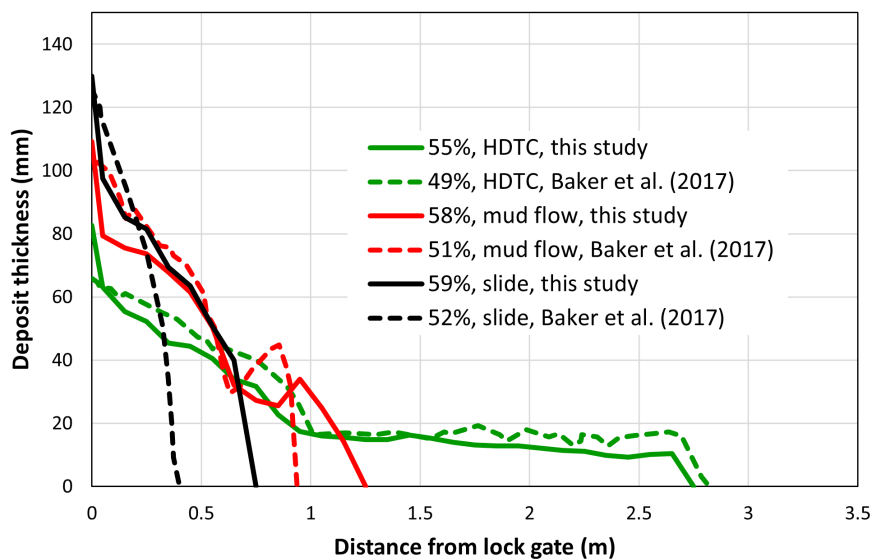

FIGURE 9 Deposit thickness of mud-grade calcite and silica-flour flows plotted against downflow distance from the lock gate, comparing selected high-density turbidity currents (HDTCs), mud flows and slides from this study and Baker et al. (2017).

anticipated that, purely from the perspective of the lack of physical cohesion, SGFs laden with mud-grade calcite on coral reefs are as effective in transporting suspended sediment as in the experiments. This includes sediment eroded and resuspended by storms and hurricanes and sediment made available by slope failures on oversteepened reef fronts and forereefs. The latter process is facilitated by the usually steep seaward slope gradient of coral reefs. As in non-carbonate environments, relatively low-concentration turbidity currents of high mobility are more likely to occur than hyperconcentrated (more than 50% by volume of suspended sediment) turbulence-suppressed mud flows and slides of low mobility on and around coral reefs. However, there are conditions in which low-mobility flows might form. Natural SGFs can be highly stratified, with suspended sediment concentrations significantly greater near the bottom of the flow than near the top, as shown for siliciclastic flows in the Congo Canyon (Azpiroz-Zabala

et al., 2017). This may take equivalent calciclastic SGFs on coral reefs into the non-turbulent, frictional regime near the seabed. Moreover, failure of unstable slopes—particularly involving 'en masse' erosion by, for example, delamination (Eggenhuisen et al., 2011)—may initiate mud flows or slides. Notwithstanding these conditions, the lack of physical cohesion should promote the transport of suspended fine-grained $CaCO_3$ away from reefs by SGFs and thus the efficiency of cleansing turbid water after storms, so more light is available for photosynthesis. This removal of suspended sediment is probably even more effective above unhealthy reefs than above healthy reefs, because the increased volume of biologically produced mud-grade calcite on unhealthy, brittle reefs (MacDonald & Perry, 2003; Perry et al., 2015; Russ et al., 2015), as well as the greater potential for sediment erosion during storms, are expected to increase the suspended sediment concentration and thus the excess density and mobility of SGFs.

However, physical cohesion is not the only parameter that controls the mobility of $CaCO_3$-laden SGFs. Biological cohesion associated with 'sticky' extracellular polymeric substances (EPS) produced by microphytobenthos, bacteria and other micro-organisms, has been found to reduce the mobility of SGFs at concentrations that are several orders of magnitude lower than for physically cohesive, siliciclastic clay (Craig et al., 2020; Sobocinska & Baas, 2022). Coral reefs are characterised by a large species richness and diversity and carbonate grains coated in organic matter are common (Schieber et al., 2013). It is therefore probable that EPS hinder the removal of suspended sediment by SGFs from reefs by increasing the cohesive forces and attenuating the turbulent driving forces, especially in high-density turbidity currents. On unhealthy reefs, microbial films and algae grow rapidly, outcompeting corals for space (Tanner, 1995; Lirman, 2001; Barott et al., 2011), and producing large volumes of EPS. This is postulated to further reduce the mobility of SGFs above and around unhealthy reefs and thus reduce the potential to transport suspended sediment away from these compared to healthy reefs. This reduced mobility around unhealthy reefs would work against the increased mobility by the lack of physical cohesion, inferred above. Despite the conceivable reduction in SGF mobility by biological cohesion, Hubbard (1986) showed that 1/3 to 1/2 of the annual offshore sediment flux can be reached during merely two weeks of stormy weather. This supports the strong influence of physical conditions on offshore sediment transport in carbonate environments.

In addition to biological cohesion, particle shape and density also need to be considered in assessing the mobility of $CaCO_3$-laden SGFs and their ability to clean turbid water (de Kruijf et al., 2021; Bian et al., 2023). The mud-grade calcite used in the present experiments is not ideal for studying these parameters. It consists of finely powdered limestone that is suitable for understanding the basic physical properties of mud-grade calcite SGFs, but it may not represent the perceived compositional and textural variability of natural flows. Although the density of $CaCO_3$ is comparable to that of quartz-rich siliciclastic sediment, the true density of carbonate particles in natural environments is controlled by the internal porosity of bioclasts; most bioclasts have a density below $2710\,kg\,m^{-3}$. The shape of bioclasts is also more variable than the shape of siliciclastic particles. Whereas siliciclastic particles usually approach a spherical shape, the shape of bioclastic particles ranges from spherical for ooids to highly irregular, depending on the shape of shells, skeletons and other hard parts of calcifying organisms, and fragments thereof (de Kruijf et al. 2021). Moreover, mud to silt-grade carbonate produced in tropical reef environments is excreted by fish (Salter et al., 2012) and may have a range of shapes as well as disaggregation potential (Perry et al., 2011). Based on detailed laboratory experiments, Slootman et al. (2023) showed that natural non-spheroidal skeletal carbonate sand generally has a lower settling velocity than spheroidal sand. This implies that SGFs laden with non-spherical carbonate sand have a higher mobility than SGFs with spherical sand, especially if the sand particles are porous. However, further research is needed to test if the results of Slootman et al. (2023) extend to SGFs laden with clay and silt-sized $CaCO_3$.

The benefits of the perceived highly mobile nature of SGFs laden with mud-grade calcite may extend beyond the cleansing of turbid water above shallow-water reefs that depend primarily on photosynthesis. Deep-water reefs, including reefs in canyons, exist in the mesophotic zone (30–150 m; Lesser et al., 2009), where removing suspended sediment is not as vital as for shallow-water reefs. Deep-water reefs rely less on sunlight for photosynthesis and more on nutrient supply (heterotrophy rather than autotrophy; Mass et al., 2007). Hence, the high mobility of mud-grade calcite SGFs makes them effective as export systems of sediment from shallow-water reefs, and also as import systems of nutrients to deep-water reefs. Given the recently discovered common occurrence of SGFs (Azpiroz-Zabala et al., 2017) and other types of currents, such as tidal currents, in canyons, this process of nutrient supply to deep-water reefs may be more important than realised previously, and therefore add to better known nutrient sources of pelagic and deep-water bottom-current origin.

6 | CONCLUSIONS

The present experimental research reveals that SGFs laden with mud-grade calcite are non-cohesive and behave in a similar way to SGFs laden with non-cohesive siliciclastic fine silt. Both flow types remain fully turbulent and highly mobile up to concentrations that approach those of randomly packed deposits, reflected in similar maximum head velocity curves and suspended-sediment-concentration controlled run-out distances and deposit thicknesses. Reduced mobility in hyperconcentrated mud-grade calcite SGFs involves frictional forces, which require particles to be close enough to rub against each other and thereby take forward energy out of the flow. However, the 50% or more of fine $CaCO_3$ required for frictional forces to become effective are less probable in nature than the lower concentrations at which turbulent forces dominate mud-grade calcite flows. It is therefore concluded that, purely from the

perspective of the lack of physical cohesion, mud-grade calcite SGFs should be highly effective in moving suspended sediment away from shallow-water reefs, especially if a slope is present, such as on the reef front and forereef.

This study provides a platform for further increases in the understanding of SGFs laden with fine $CaCO_3$ by incorporating the influence of biological cohesion, particle density and particle shape on the sediment transport dynamics of SGFs above and around coral reefs and in other carbonate environments. Given the high ecological, economic and societal importance of coral reefs and the threat imposed to reefs by anthropogenic climate change, a redressing of the balance between studies of siliciclastic and calciclastic SGFs in favour of calciclastic SGFs and their deposits is timely.

CONFLICT OF INTEREST STATEMENT

The authors have no conflict of interest to declare.

DATA AVAILABILITY STATEMENT

The data that support the findings of this study are available from the corresponding author upon reasonable request.

ORCID

Jaco H. Baas https://orcid.org/0000-0003-1737-5688
Stephen Lokier https://orcid.org/0000-0001-5845-410X
James Hendry https://orcid.org/0000-0002-8448-6057

REFERENCES

Anthony, K.R.N., Kline, D.I., Diaz-Pulido, G., Dove, S. & Hoegh-Guldberg, O. (2008) Ocean acidification causes bleaching and productivity loss in coral reef builders. *Proceedings of the National Academy of Sciences of the United States of America*, 105(45), 17442–17446.

Austin, J., Schlager, W. & Palmer, A. (1986) *Leg 101: proceedings Initial Reports (Pt A)*. College Station, TX: Ocean Drilling Program.

Azpiroz-Zabala, M., Cartigny, M.J.B., Talling, P.J., Parsons, D.R., Sumner, E.J., Clare, M.A., Simmons, S.M., Cooper, C. & Pope, E.L. (2017) Newly recognized turbidity current structure can explain prolonged flushing of submarine canyons. *Science Advances*, 3, e1700200.

Baas, J.H. & Best, J.L. (2002) Turbulence modulation in clay-rich sediment-laden flows and some implications for sediment deposition. *Journal of Sedimentary Research*, 72, 336–340.

Baas, J.H., Best, J.L. & Peakall, J. (2011) Depositional processes, bedform development and hybrid bed formation in rapidly decelerated cohesive (mud–sand) sediment flows. *Sedimentology*, 58, 1953–1987.

Baas, J.H., Best, J.L., Peakall, J. & Wang, M. (2009) A phase diagram for turbulent, transitional, and laminar clay suspension flows. *Journal of Sedimentary Research*, 79, 162–183.

Baker, M.L. & Baas, J.H. (2023) Does sand promote or hinder the mobility of cohesive sediment gravity flows? *Sedimentology*, 70, 1110–1130.

Baker, M.L., Baas, J.H. & Malarkey, J. (2017) The effect of clay type on the properties of cohesive sediment gravity flows and their deposits. *Journal of Sedimentary Research*, 87, 1176–1195.

Barott, K.L., Rodriguez-Mueller, B., Youle, M., Marhaver, K.L., Vermeij, M.J.A., Smith, J.E. & Rohwer, F.L. (2011) Microbial to reef scale interactions between the reef-building coral Montastraea annularis and benthic algae. *Proceedings of the Royal Society B: Biological Sciences*, 279, 1655–1664.

Berkelmans, R. & van Oppen, M.J.H. (2006) The role of zooxanthellae in the thermal tolerance of corals: a 'nugget of hope' for coral reefs in an era of climate change. *Proceedings of the Royal Society B*, 273, 2305–2312.

Betzler, C., Eberli, G.P. & Alvarez Zarikian, C.A. (2017) Maldives monsoon and sea level. Proceedings of the International Ocean Discovery Program, 359, College Station, TX.

Bian, C., Chen, J., Jiang, C., Wu, Z. & Yao, Z. (2023) Threshold of motion of coral sediment under currents in flume experiments. *Sedimentology*, 70, 1723–1740.

Brodie, J. & Pearson, R.G. (2016) Ecosystem health of the Great Barrier Reef: time for effective management action based on evidence. *Estuarine, Coastal and Shelf Science*, 183, 438–451.

Brunner, C.A. (2021) Climate change doubles sedimentation-induced coral recruit mortality. *Science of the Total Environment*, 768, 143897.

Chazottes, V., Reijmer, J.J.G. & Cordier, E. (2008) Sediment characteristics in reef areas influenced by eutrophication-related alterations of benthic communities and bioerosion processes. *Marine Geology*, 250, 114–127.

Cinner, J. (2014) Coral reef livelihoods. *Current Opinion in Environmental Sustainability*, 7, 65–71.

Costanza, R., de Groot, R., Sutton, P., van der Ploeg, S., Anderson, S.J., Kubiszewski, I., Farber, S. & Turner, R.K. (2014) Changes in the global value of ecosystem services. *Global Environmental Change*, 26, 152–158.

Craig, M.J., Baas, J.H., Amos, K.J., Strachan, L.J., Manning, A.J., Paterson, D.M., Hope, J.A., Nodder, S.D. & Baker, M.L. (2020) Biomediation of submarine sediment gravity flow dynamics. *Geology*, 48, 72–76.

Crook, E.D., Cohen, A.L., Rebolledo-Vieyra, M., Hernandez, L. & Paytan, A. (2013) Reduced calcification and lack of acclimatization by coral colonies growing in areas of persistent natural acidification. *Proceedings of the National Academy of Sciences of the United States of America*, 110, 11044–11049.

de Kruijf, M., Slootman, A., de Boer, R.A. & Reijmer, J.J.G. (2021) On the settling of marine carbonate grains: review and challenges. *Earth-Science Reviews*, 217, 103532.

Dyer, K.R. & Manning, A.J. (1999) Observation of the size, settling velocity and effective density of flocs, and their fractal dimensions. *Journal of Sea Research*, 41, 87–95.

Eberli, G.P. (1987) Carbonate turbidite sequences deposited in rift-basins of the Jurassic Tethys Ocean (eastern Alps, Switzerland). *Sedimentology*, 34, 363–388.

Eberli, G.P., Swart, P.K. & Malone, M.J. (1997) Proceedings Ocean Drilling Program. Initial Reports, Leg 166, College Station, TX, p. 850.

Eggenhuisen, J.T., McCaffrey, W.D., Haughton, P.D.W. & Butler, R.W.H. (2011) Shallow erosion beneath turbidity currents and its impact on the architectural development of turbidite sheet systems. *Sedimentology*, 58, 936–959.

Erftemeijer, P.L.A., Riegl, B., Hoeksema, B.W. & Todd, P.A. (2012) Environmental impacts of dredging and other sediment disturbances on corals: a review. *Marine Pollution Bulletin*, 64, 1737–1765.

Eriksson, R., Merta, J. & Rosenholm, J.B. (2007) The calcite/water interface: I. Surface charge in indifferent electrolyte media and the influence of low-molecular-weight polyelectrolyte. *Journal of Colloid and Interface Science*, 313, 184–193.

Evans, R.D., Wilson, S.K., Fisher, R., Ryan, N.M., Babcock, R., Blakeway, D., Bond, T., Dorji, P., Dufois, F., Fearns, P., Lowe, R.J., Stoddart, J. & Thomson, D.P. (2020) Early recovery dynamics of turbid coral reefs after recurring bleaching events. *Journal of Environmental Management*, 268, 110666.

Folk, R.L. & Ward, W.C. (1957) Brazos river bar: a study in the significance of grain size parameters. *Journal of Sedimentary Petrology*, 27, 3–26.

Gattuso, J.P., Allemand, D. & Frankignoulle, M. (1999) Photosynthesis and calcification at cellular, organismal and community levels in coral reefs: a review on interactions and control by carbonate chemistry. *American Zoologist*, 39, 160–183.

Haak, A.B. & Schlager, W. (1989) Compositional variations in calciturbidites due to sea-level fluctuations, late Quaternary, Bahamas. *Geologische Rundschau*, 78, 477–486.

Hodson, J.M. & Alexander, J. (2010) The effects of grain density variation on turbidity currents and some implications for the deposition of carbonate turbidites. *Journal of Sedimentary Research*, 80, 515–528.

Hubbard, D.K. (1986) Sedimentation as a control of reef development: St. Croix, U.S.V.I. *Coral Reefs*, 5, 117–125.

Hubbard, D.K., Miller, A.I. & Scaturo, D. (1990) Production and cycling of calcium carbonate in a shelf-edge reef system (St. Croix, US Virgin Islands); Applications to the nature of reef systems in the fossil record. *Journal of Sedimentary Petrology*, 60, 335–360.

Hughes, T.P., Anderson, K.D., Connolly, S.R., Heron, S.F., Kerry, J.T., Lough, J.M., Baird, A.H., Baum, J.K., Berumen, M.L., Bridge, T.C., Claar, D.C., Eakin, C.M., Gilmour, J.P., Graham, N.A.J., Harrison, H., Hobbs, J.-P.A., Hoey, A.S., Hoogenboom, M., Lowe, R.J., McCulloch, M.T., Pandolfi, J.M., Pratchett, M., Schoepf, V., Torda, G. & Wilson, S.K. (2018) Spatial and temporal patterns of mass bleaching of corals in the Anthropocene. *Science*, 359, 80–83.

Jones, R., Giofre, N., Luter, H.M., Neoh, T.L., Fisher, R. & Duckworth, A. (2020) Responses of corals to chronic turbidity. *Scientific Reports*, 10, 4762.

Kneller, B. & Buckee, C. (2000) The structure and fluid mechanics of turbidity currents: a review of some recent studies and their geological implications. *Sedimentology*, 47, 62–94.

Langdon, C. & Atkinson, M.J. (2005) Effect of elevated pCO_2 on photosynthesis and calcification of corals and interactions with seasonal change in temperature/irradiance and nutrient enrichment. *Journal of Geophysical Research: Oceans*, 110, C09S07.

Lesser, M.P., Slattery, M. & Leichter, J.J. (2009) Ecology of mesophotic coral reefs. *Journal of Experimental Marine Biology and Ecology*, 375, 1–8.

Lirman, D. (2001) Competition between macroalgae and corals: effects of herbivore exclusion and increased algal biomass on coral survivorship and growth. *Coral Reefs*, 19, 392–399.

Liu, G., Wang, D., Chen, W., Wang, W., Betzler, C. & Han, X. (2023) Submarine landslides on a carbonate platform slope changing transport pathways of deepwater gravity flows: insights from the Xisha Islands, South China Sea. *Geomorphology*, 437, 108813.

Lokier, S.W. (2023) Marine carbonate sedimentation in volcanic settings. In: Di Capua, A., De Rosa, R., Kereszturi, G., Le Pera, E., Rosi, M. & Watt, S.F.L. (Eds) *Volcanic processes in the sedimentary record: when volcanoes meet the environment. Geological Society of London, Special Publication*, 520, 547–594.

Lokier, S.W., Wilson, M.E.J. & Burton, L.M. (2009) Marine biota response to clastic sediment influx: a quantitative approach. *Palaeogeography, Palaeoclimatology, Palaeoecology*, 281, 25–42.

Lopez-Gamundi, C., Barnes, B.B., Bakker, A.C., Harris, P., Eberli, G.P. & Purkis, S.J. (2024) Spatial, seasonal, and climatic drivers of suspended sediment atop Great Bahama Bank. *Sedimentology*, 71, 769–792.

MacDonald, I.A. & Perry, C.T. (2003) Biological degradation of coral framework in a turbid lagoon environment, Discovery Bay, north Jamaica. *Coral Reefs*, 22, 523–535.

Mallela, J. & Perry, C.T. (2006) Calcium carbonate budgets for two coral reefs affected by different terrestrial runoff regimes, Rio Bueno, Jamaica. *Coral Reefs*, 26, 129–145.

Marr, J.G., Harff, P.A., Shanmugam, G. & Parker, G. (2001) Experiments on subaqueous sandy gravity flows: the role of clay and water content in flow dynamics and depositional structures. *Geological Society of America Bulletin*, 113, 1377–1386.

Mass, T., Einbinder, S., Brokovich, E., Shashar, N., Vago, R., Erez, J. & Dubinsky, Z. (2007) Photoacclimtion of Stylophora pistillata to light extremes: metabolism and calcification. *Marine Ecology Progress Series*, 334, 93–102.

Mehta, A.J., Hayter, E.J., Parker, R., Krone, R.B. & Teeter, A.M. (1989) Cohesive sediment transport. 1: process description. *Journal of Hydraulic Engineering*, 115, 1076–1093.

Middleton, G.V. & Hampton, M.A. (1973) Part 1. Sediment gravity flows: mechanics of flow and deposition. In: Middleton, G.V. & Bouma, A.A. (Eds.) *Turbidites and deep-water sedimentation*. Anaheim, CA: SEPM Pacific Section Short Course Notes, p. 38.

Mohrig, D. & Marr, J.G. (2003) Constraining the efficiency of turbidity current generation from submarine debris flows and slides using laboratory experiments. *Marine and Petroleum Geology*, 20, 883–899.

Mulder, T. & Alexander, J. (2001) The physical character of subaqueous sedimentary density flow and their deposits. *Sedimentology*, 48, 269–299.

Parker, G. (1987) Experiments on turbidity currents over an erodible bed. *Journal of Hydraulic Research*, 25, 123–147.

Pashley, R.M. & Karaman, M.E. (2004) *Applied Colloid and Surface Chemistry*. London: John Wiley & Sons, p. 188.

Payros, A. & Pujalte, V. (2008) Calciclastic submarine fans: an integrated overview. *Earth-Science Reviews*, 86, 203–246.

Perry, C.T., Salter, M.A., Harborne, A.R., Crowley, S.F., Jelks, H.L. & Wilson, R.W. (2011) Fish as major carbonate mud producers and missing components of the carbonate factory. *Proceedings of the National Academy of Sciences of the United States of America*, 108, 3865–3869.

Perry, C.T., Kench, P.S., O'Leary, M.J., Morgan, K.M. & Januchowski-Hartley, F. (2015) Linking reef ecology to Island building: parrotfish identified as major producers of Island-building sediment in the Maldives. *Geology*, 43, 503–506.

Postma, G. (2011) Sediment gravity flow. In: Singh, V.P., Singh, P. & Haritashya, U.K. (Eds.) *Encyclopedia of snow, ice and glaciers*, Geology Faculty Publications, Paper 7. Dayton, OH: University of Dayton, pp. 1005–1010.

Reijmer, J.J.G., Palmieri, P. & Groen, R. (2012) Compositional variations in calciturbidites and calcidebrites in response to sea-level fluctuations (Exuma Sound, Bahamas). *Facies*, 58, 493–507.

Reijmer, J.J.G., Schlager, W., Bosscher, H., Beets, C.J. & McNeill, D.F. (1992) Pliocene/Pleistocene platform facies transition recorded in calciturbidites (Exuma Sound, Bahamas). *Sedimentary Geology*, 78, 171–179.

Rogers, C.S. & Ramos-Scharrón, C.E. (2022) Assessing effects of sediment delivery to coral reefs: a Caribbean watershed perspective. *Frontiers in Marine Science*, 8, 773968.

Rogers, C.S. (1990) Responses of coral reefs and reef organisms to sedimentation. *Marine Ecology Progress Series*, 62, 185–202.

Russ, G.R., Questel, S.L.A., Rizzari, J.R. & Alcala, A.C. (2015) The parrotfish–coral relationship: refuting the ubiquity of a prevailing paradigm. *Marine Biology*, 162, 2029–2045.

Salter, M.A., Perry, C.T. & Wilson, R.W. (2012) Production of mud-grade carbonates by marine fish: crystalline products and their sedimentary significance. *Sedimentology*, 59, 2172–2198.

Schieber, J., Southard, J.B., Kissling, P., Rossman, B. & Ginsburg, R. (2013) Experimental deposition of carbonate mud from moving suspensions: importance of flocculation and implications for modern and ancient carbonate mud deposition. *Journal of Sedimentary Research*, 83, 1025–1031.

Scoffin, T. (1993) The geological effects of hurricanes on coral reefs and the interpretation of storm deposits. *Coral Reefs*, 12, 203–221.

Sheppard, C., Davy, S., Pilling, G. & Graham, N. (2017) *The Biology of Coral Reefs*. Oxford: Oxford University Press, p. 384.

Slootman, A., de Kruijf, M., Glatz, G., Eggenhuisen, J.T., Zühlke, R. & Reijmer, J.J.G. (2023) Shape-dependent settling velocity of skeletal carbonate grains: implications for calciturbidites. *Sedimentology*, 70, 1683–1722.

Sobocinska, A. & Baas, J.H. (2022) Effect of biological polymers on mobility and run-out distance of cohesive and non-cohesive sediment gravity flows. *Marine Geology*, 452, 106904.

Spalding, M.D. (2001) *World Atlas of Coral Reefs*. Berkeley, CA: University of California Press, p. 424.

Spalding, M.D., Ruffo, S., Lacambra, C., Meliane, I., Hale, L., Shepard, C.C. & Beck, M.W. (2014) The role of ecosystems in coastal protection: adapting to climate change and coastal hazards. *Ocean and Coastal Management*, 90, 50–57.

Stocker, T.F., Qin, D., Plattner, G.-K., Tignor, M., Allen, S.K., Boschung, J., Nauels, A., Xia, Y., Bex, V. & Midgley, P.M. (2013) *Climate change 2013: the physical science basis. Contribution of working group I to the fifth assessment report of the Intergovernmental Panel on Climate Change*. Cambridge and New York, NY: Cambridge University Press, p. 1535.

Sumner, E.J., Talling, P.J. & Amy, L.A. (2009) Deposits of flows transitional between turbidity current and debris flow. *Geology*, 37, 991–994.

Swart, P.K., Eberli, G.P., Malone, M.J. & Sarg, J.F. (2000) *Proceedings Ocean Drilling Program, Leg 166, Scientific Results*. College Station, TX: Ocean Drilling Program, p. 213.

Talling, P.J. (2014) On the triggers, resulting flow types and frequencies of subaqueous sediment density flows in different settings. *Marine Geology*, 352, 155–182.

Talling, P.J., Allin, J., Armitage, D.A., Arnott, R.W.C., Cartigny, M.J.B., Clare, M.A., Felletti, F., Covault, J.A., Girardclos, S., Hansen, E., Hill, P.R., Hiscott, R.N., Hogg, A.J., Clarke, J.H., Jobe, Z.R., Malgesini, G., Mozzato, A., Naruse, H., Parkinson, S., Peel, F.J., Piper, D.J.W., Pope, E., Postma, G., Rowley, P., Sguazzini, A., Stevenson, C.J., Sumner, E.J., Sylvester, Z., Watts, C. & Xu, J. (2015) Key future directions for research on turbidity currents and their deposits. *Journal of Sedimentary Research*, 85, 153–169.

Talling, P.J., Masson, D.G., Sumner, E.J. & Malgesini, G. (2012) Subaqueous sediment density flows: depositional processes and deposit types. *Sedimentology*, 59, 1937–2003.

Tanner, J.E. (1995) Competition between scleractinian corals and macroalgae: an experimental investigation of coral growth, survival and reproduction. *Journal of Experimental Marine Biology and Ecology*, 190, 151–168.

Trower, E.J., Lamb, M.P. & Fischer, W.W. (2019) The origin of carbonate mud. *Geophysical Research Letters*, 46, 2696–2703.

Tuttle, L.J. & Donahue, M.J. (2022) Effects of sediment exposure on corals: a systematic review of experimental studies. *Environmental Evidence*, 11(4), 33.

Venn, A.A., Tambutté, E., Caminiti-Segonds, N., Techer, N., Allemand, D. & Tambutté, S. (2019) Effects of light and darkness on pH regulation in three coral species exposed to seawater acidification. *Scientific Reports*, 9, 2201.

Wilson, M.E.J. (2012) Equatorial carbonates: an earth systems approach. *Sedimentology*, 59, 1–31.

SUPPORTING INFORMATION

Additional supporting information can be found online in the Supporting Information section at the end of this article.

How to cite this article: Baas, J.H., Hewitt, W., Lokier, S. & Hendry, J. (2024) Coming to light: How effective are sediment gravity flows in removing fine suspended carbonate from reefs? *The Depositional Record*, 00, 1–16. Available from: https://doi.org/10.1002/dep2.319